International Journal of Multiphysics
Volume 19, No. 1, 2025
ISSN: 1750-9548

Thermoacoustic Heat Transfer in a Cylinder under Non-Uniform Thermal Flow

Fatemeh Sobhnamayan[1], Faramarz Sarhaddi[1*], Amin Behzadmehr[1]

[1] Department of Mechanical Engineering, University of Sistan and Baluchestan, Zahedan, Iran

*Corresponding author

Abstract

In this paper, the effect of non-uniform main thermal flow on thermoacoustic heat transfer in a cylinder is investigated. In order to model thermoacoustic phenomenon, the hydrodynamic and thermal parameters of the flow are considered as the decomposition of a main flow and oscillating flow. The general and particular governing equations, including continuity, momentum, energy, and the ideal gas law, are developed assuming transient two-dimensional viscous flow in cylindrical coordinate. Various functions (linear, exponential, logarithmic, sine, and Bessel) are considered for the main flow temperature. From the simplification of the governing equations, a series of ordinary differential equations have been obtained, which have been solved semi-analytically. The semi-analytical results of the present study are in good agreement with the analytical results of previous studies. The results of the present study show that the logarithmic temperature function for the main flow provides the highest gain of work flux density. However, the linear temperature function also provides a relatively good gain and can be created more easily than the logarithmic function.

Keywords: Thermoacoustic heat transfer; Cylinder; Non-uniform thermal flow.

Introduction

Thermoacoustics is a branch of engineering science that studies the interactions between thermal and acoustic phenomena. It focuses specifically on how sound waves are generated by temperature differences, as well as the effect of sound waves on temperature distribution and heat transfer. The application of thermoacoustic principles is observed in various fields, including engineering, environmental sciences, and even medical technology. In a thermoacoustic system, a temperature gradient generates a sound wave, and the sound wave causes pressure oscillations and work production. Thermoacoustic systems have advantages such as simplicity of structure and the ability to use low-grade energy sources (solar energy, waste heat, etc.). However, their energy conversion efficiency is not very high. Therefore, it is essential to study ways to increase their energy conversion efficiency. Various experimental and theoretical research has been conducted on modeling the basic principles of thermoacoustic phenomenon and its applications, some of which will be reviewed below.

Kramers (1949) modeled thermoacoustic oscillations in a closed-ended cylinder under temperature gradient using boundary layer theory [1]. His modeling results differed greatly from experimental observations. From his results, it can be concluded that boundary layer theory is not a suitable tool for modeling thermoacoustic phenomenon. Rott (1969) developed a new theory for analyzing thermoacoustic phenomenon assuming transient two-dimensional viscous flow [2]. His theory involved the decomposition of a main thermal flow and thermoacoustic oscillations. Rott's theory is currently used to analyze thermoacoustic heat transfer in many practical applications. Wu et al. (2001) investigated the thermoacoustic heat transfer of a ferromagnetic fluid under an external magnetic field [3]. They pointed out that heat transfer in a ferromagnetic fluid can be improved by generating a thermoacoustic wave and a magnetic field. Dai et al. (2006) presented a method for determining the optimal operating frequency of thermoacoustic systems based on linear acoustic wave theory [4]. Their results showed that there is a turning point for the volume flow rate that optimizes the system operating frequency. This turning point is located at the boundary of the flow velocity node. Tasnim et al. (2011) modeled thermoacoustic flow and heat transfer in a porous medium [5]. They used the Brinkman-Forchheimer extended Darcy model and obtained analytical expressions for the oscillating velocity and temperature and energy flux density. The analytical results of their research provide a useful tool for designing porous media (stacks) in thermoacoustic systems. Kam et al. (2016) simulated the propagation of thermoacoustic wave in a two-dimensional enclosure [6]. They solved the Navier-Stokes equations using a combined finite difference method and a lattice Boltzmann network. Compared to conventional linear analytical solutions, the numerical solution carried out has higher accuracy and can take into account the nonlinear effects of thermoacoustic wave propagation. Gant et al. (2021) numerically investigated the effect of time delay and noise on an inviscid thermoacoustic wave [7]. Their results show that the presence of a time delay in the thermoacoustic model preserves the intrinsic thermoacoustic states in the dynamic behavior of the system. Also, including noise in the thermoacoustic model provides a more realistic dynamic behavior of the thermoacoustic system performance. Liu et al. (2022) studied the intrinsic thermoacoustic instabilities in thermoacoustic systems [8]. The main instability factors include acoustic disturbances, flow oscillations, and pulsation of heat release. They pointed out that even if acoustic disturbances are removed from the thermoacoustic system, thermoacoustic instabilities due to the fluctuations of flow and heat transfer still exist. Yang et al. (2023) theoretically investigated the thermoacoustic flow and heat transfer of a plasma fluid under a magnetic field [9]. Their research results provide basic concepts for the design of closed-cycle MHD generators. Blanc and Ramon (2024) studied the thermoacoustic flow and heat transfer in a radiant energy absorbing medium theoretically [10]. Their research results showed that radiation-driven thermoacoustic systems have higher performance than conventional thermoacoustic systems. They also pointed out that the performance of radiation-driven thermoacoustic systems is highly dependent on the matching of the heat time delay and the acoustic oscillations period. Huang et al. (2025) simulated the effect of axial structural vibrations on the dynamic behavior of thermoacoustic systems [11]. They solved the nonlinear governing equations of the problem using the large eddy simulation method. Their research results provide in-depth knowledge regarding the interaction between intrinsic thermoacoustic instabilities and axial structural vibrations in thermoacoustic systems. Misra and Banerjee (2025) theoretically studied how thermoacoustic shocks form in complex plasma flows [12]. They solved the Bateman-Burgers equations in the presence of a series of nonlinear terms related to the motion of charged particles in the plasma. Their results include investigating the effect of various parameters including thermal diffusion, thermal feedback, heat capacity, viscosity and particle collision on thermoacoustic shocks. Merk et al. (2025) introduced a new framework based on the Jacobian method to predict the dynamic behavior of thermoacoustic waves under jump conditions [13]. Their proposed framework has the ability to predict the dynamic behavior of thermoacoustic waves under various physical conditions, including different Mach numbers, real gas properties, combined and entropic oscillations, etc. In previous researches [1-13], the effect of various design and operating parameters on thermoacoustic flow and heat transfer has been investigated. However, the effect of non-uniform main thermal flow on the dynamic behavior of thermoacoustic waves has not been investigated. Investigating the effect of the main thermal flow type can provide new ideas for improving the process of thermoacoustic heat transfer. Therefore, in the present study, various functions (linear, exponential, logarithmic, sine, and Bessel) are considered for the main flow temperature, and then their effect on the thermoacoustic parameters of the flow and heat transfer is investigated.

Governing equations

The geometry of the problem is shown in Fig. 1.

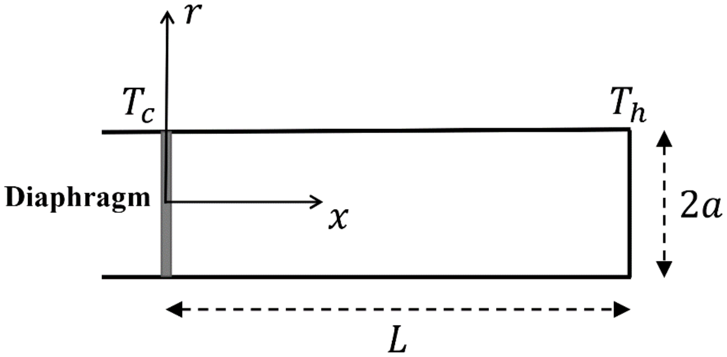

Fig. 1. Geometry of the problem

Where T_c, T_h, a and L, are temperature of heat sink, temperature of heat source, radius of cylinder and length of cylinder, respectively. The governing equations for thermoacoustic phenomenon include continuity, momentum, energy, and the ideal gas law, which is written in the cylindrical coordinate system as follows

Continuity:

$$\frac{\partial \rho}{\partial t} + \frac{1}{r}\frac{\partial}{\partial r}(\rho r v) + \frac{\partial}{\partial x}(\rho u) = 0 \tag{1}$$

x- momentum:

$$\rho \frac{\partial u}{\partial t} + \frac{\partial p}{\partial x} = \mu \frac{1}{r}\frac{\partial}{\partial r}\left(r \frac{\partial u}{\partial r}\right) \tag{2}$$

r- momentum:

$$\frac{\partial p}{\partial r} = 0 \tag{3}$$

Energy:

$$\rho c_p \left(\frac{\partial T}{\partial t} + u \frac{\partial T}{\partial x}\right) = \frac{1}{r}\frac{\partial}{\partial r}\left(kr \frac{\partial T}{\partial r}\right) + \beta T \frac{\partial p}{\partial t} \tag{4}$$

The ideal gas law:

$$p = \rho R T \tag{5}$$

Where u, v, T, p, ρ, c_p, k, μ and β are axial component of thermoacoustic velocity, radial component of thermoacoustic velocity, thermoacoustic temperature, thermoacoustic pressure, thermoacoustic density, specific heat capacity, thermal conductivity, dynamic viscosity and coefficient of volumetric thermal expansion, respectively. The thermoacoustic flow parameters are defined from the decomposition of the main flow parameters and thermoacoustic oscillations as follows [2, 5]

$$u(r,x,t) = u'(r,x)e^{i\omega t} \tag{6}$$

$$v(r,x,t) = v'(r,x)e^{i\omega t} \tag{7}$$

$$\rho(r,x,t) = \rho_m(x) + \rho'(r,x)e^{i\omega t} \tag{8}$$

$$T(r,x,t) = T_m(x) + T'(r,x)e^{i\omega t} \tag{9}$$

$$p(x,t) = \underbrace{p_m}_{\text{cte}} + p'(x)e^{i\omega t} \tag{10}$$

Here, the quantities indicated by the subscript "m" are the main flow parameters. Using the concept of linearization and substituting the thermoacoustic parameters of Eqs. (6)-(10) into Eqs. (1)-(5), the following equations are obtained [2]

$$i\omega\rho' + \rho_m \frac{1}{r}\frac{\partial}{\partial r}(rv') + \rho_m \frac{\partial u'}{\partial x} + u' \frac{\partial \rho_m}{\partial x} = 0 \tag{11}$$

$$i\omega u' + \frac{1}{\rho_m}\frac{dp'}{dx} = \vartheta \frac{1}{r}\frac{\partial}{\partial r}\left(r \frac{\partial u'}{\partial r}\right) \tag{12}$$

$$\rho_0 c_p \left(i\omega T' + u' \frac{dT_0}{dx}\right) = \frac{1}{r}\frac{\partial}{\partial r}\left(kr \frac{\partial T'}{\partial r}\right) + i\omega p' \tag{13}$$

$$T' = \frac{p'}{R\rho_m} - \frac{\rho' T_m}{\rho_m} \tag{14}$$

Where ω, ϑ and R are angular frequency, kinematic viscosity and gas constant, respectively. Eq. (12) can be rewritten in the following form

$$\begin{cases}\frac{\partial^2 u'}{\partial r^2}+\frac{1}{r}\frac{\partial u'}{\partial r}-\eta^2 u'=\frac{1}{\vartheta\rho_m}\frac{dp'}{dx}\\ u'(0,x)=\text{finite}\\ u'(a,x)=0\end{cases} \tag{15}$$

Here $\eta^2 = i\omega/\vartheta$. The oscillating velocity is obtained from solving Eq. (15) as follows

$$u'(r,x)=\frac{i}{\rho_m\omega}\frac{dp'}{dx}\left(1-\frac{I_0(\eta r)}{I_0(\eta a)}\right) \tag{16}$$

The radial average of oscillating velocity is introduced as follows

$$\overline{u'}(x)=\int_{r=0}^{r=a} u'(r,x)2\pi r dr=\frac{2\pi i}{\rho_m\omega}\frac{dp'}{dx}\left(\frac{a^2}{2}-\frac{aI_1(\eta a)}{\eta I_0(\eta a)}\right) \tag{17}$$

Here, I_0 and I_1 are the modified Bessel functions of the first kind, of order zero and order one, respectively. Combining Eq. (13) and (14), a partial differential equation for the oscillating density is obtained as follows

$$\begin{cases}\frac{\partial^2 \rho'}{\partial r^2}+\frac{1}{r}\frac{\partial \rho'}{\partial r}-\zeta^2\rho'=\zeta^2\left(-\rho'_w+\frac{\gamma-1}{c^2}p'\right)-\frac{\zeta^2}{\omega^2}\theta\frac{dp'}{dx}\left(1-\frac{I_0(\eta r)}{I_0(\eta a)}\right)\\ \rho'(0,x)=\text{finite}\\ \rho'(a,x)=\rho'_w\end{cases} \tag{18}$$

The oscillating density is obtained from solving Eq. (18) as follows

$$\rho'(r,x)-\rho'_w=\left(-\frac{\gamma-1}{c^2}p'+\frac{1}{1-Pr}\frac{\theta}{\omega^2}\frac{dp'}{dx}\right)\left(1-\frac{I_0(\zeta r)}{I_0(\zeta a)}\right)-\left(\frac{Pr}{1-Pr}\frac{\theta}{\omega^2}\frac{dp'}{dx}\right)\left(1-\frac{I_0(\eta r)}{I_0(\eta a)}\right) \tag{19}$$

Where c and Pr are sound wave speed and Prandtl number, respectively. Also, $\zeta^2 = i\omega Pr/\vartheta$ and $\theta=\frac{1}{T_m}\frac{dT_m}{dx}=-\frac{1}{\rho_m}\frac{d\rho_m}{dx}$. Combining Eqs. (11), (12) and (18) and taking the integral of $\int_{r=0}^{r=a}2\pi r dr$, an ordinary differential equation for the oscillating pressure is obtained as follows

$$\delta_1(x)\frac{d^2p'}{dx^2}+\delta_2(x)\frac{dp'}{dx}+\delta_3(x)p'=0 \tag{20}$$

Here $\delta_1(x)$, $\delta_2(x)$ and $\delta_3(x)$ are defined as follows

$$\delta_1(x)=\frac{c^2}{\omega^2}\left(1-\frac{2}{\eta a}\frac{I_1(\eta a)}{I_0(\eta a)}\right) \tag{21}$$

$$\delta_2(x)=\frac{d\delta_1(x)}{dx}-\frac{c^2}{\omega^2}\frac{\theta}{1-Pr}\left(\frac{2}{\zeta a}\frac{I_1(\zeta a)}{I_0(\zeta a)}-\frac{2}{\eta a}\frac{I_1(\eta a)}{I_0(\eta a)}\right) \tag{22}$$

$$\delta_3(x)=1+(\gamma-1)\frac{2}{\zeta a}\frac{I_1(\zeta a)}{I_0(\zeta a)} \tag{23}$$

From Eq. (17), using the boundary conditions $\overline{u'}(0)=\omega l$ and $\overline{u'}(L)=0$, two boundary conditions for Eq. (20) are obtained as follows [14]

$$\frac{dp'(0)}{dx}=p_1=\frac{\rho_m\omega^2 l}{2\pi i\left(\frac{a^2}{2}-\frac{aI_1(\eta a)}{\eta I_0(\eta a)}\right)} \tag{24}$$

$$\frac{dp'(L)}{dx}=0 \tag{25}$$

The work flux density is a criterion to characterize the local energy conversion of thermoacoustic process. It is defined as follows [15]

$$w(r,x)=\frac{1}{2}\mathrm{Real}\left[\widetilde{p'}u'\right] \tag{26}$$

Here, the sign of ~ shows the complex conjugate of p'. The gain of work flux density can be defined as follows [15]

$$G=\frac{w(r,x)}{w(0,0)} \tag{27}$$

In the present study, various functions have been considered for the main flow temperature, which are given in Table 1.

Table 1. Various functions for the main flow temperature

Function type	**Coefficient of *A***	**Coefficient of *B***
$T_m(x)=Ax+B$	$A=\frac{T_h-T_c}{L}$	$B=T_c$
$T_m(x)=Ae^x+B$	$A=\frac{T_h-T_c}{e^L-1}$	$B=\frac{T_ce^L-T_h}{e^L-1}$
$T_m(x)=Aln(x+1)+B$	$A=\frac{T_h-T_c}{\ln(L+1)}$	$B=T_c$
$T_m(x)=Asin(x)+B$	$A=\frac{T_h-T_c}{sin(L)}$	$B=T_c$
$T_m(x)=AJ_0(x)+B$	$A=\frac{T_h-T_c}{J_0(L)-1}$	$B=\frac{T_cJ_0(L)-T_h}{J_0(L)-1}$

Validation

The Eq. (20), is an ordinary differential equation with variable coefficients. A finite difference technique is used to solve it by bvp4c command of MATLAB [16]. In order to validate, the semi-analytical results of thermoacoustic pressure of the present research for constant main temperature ($\theta=0$) have been compared with the results of Rott [2]. Rott's ordinary differential equation for oscillating pressure is as follows [2]

$$\begin{cases}\frac{d}{dx}\left(\frac{c^2}{\omega^2}\left(1-f_j\right)\frac{dp'}{dx}\right)-\frac{c^2}{\omega^2}\frac{\left(f_j^*-f_j\right)}{1-Pr}\theta\frac{dp'}{dx}+\left(1+(\gamma-1)f_j^*\right)p'=0\\ \frac{dp'(0)}{dx}=p_1\\ \frac{dp'(L)}{dx}=0\end{cases} \tag{28}$$

Here f_j and f_j^* are defined as follows [2]

$$f_j=\frac{2}{i\eta a}\frac{J_1(i\eta a)}{J_0(i\eta a)} \tag{29}$$

$$f_j^*=\frac{2}{i\zeta a}\frac{J_1(i\zeta a)}{J_0(i\zeta a)} \tag{30}$$

For the case of $\theta=0$, the coefficients of Eq. (28) are constant, so it has an analytical solution of the following form

$$p'(x)=\frac{p_1}{\lambda}\left(\frac{cos(\lambda x)}{tan(\lambda L)}+sin(\lambda x)\right) \tag{31}$$

Here λ^2 is defined as follows

$$\lambda^2 = \frac{\omega^2}{c^2}\frac{\left(1 + (\gamma - 1)f_j^*\right)}{\left(1 - f_j\right)} \tag{32}$$

The design parameters of cylinder are given in Table 2.

Table 2. Design parameters of cylinder

Parameter	**Value**
Radius of cylinder	$a = 0.025$ m
Length of cylinder	$L = 1$ m
Diaphragm displacement	$l = 0.001$ m
Temperature of heat source	$T_h = 600$ K
Temperature of heat sink	$T_c = 300$ K
Main flow pressure	$p_m = 101$ kPa
Specific heat capacity	$c_p = 1007$ kJ/kg. K
Dynamic viscosity	$\mu = 1.87 \times 10^{-5}$ Pa. s
Prandtl number	$Pr = 0.73$
Gas constant	$R = 287$ J/kg. K

The validation results for the thermoacoustic pressure are shown in Fig. 2.

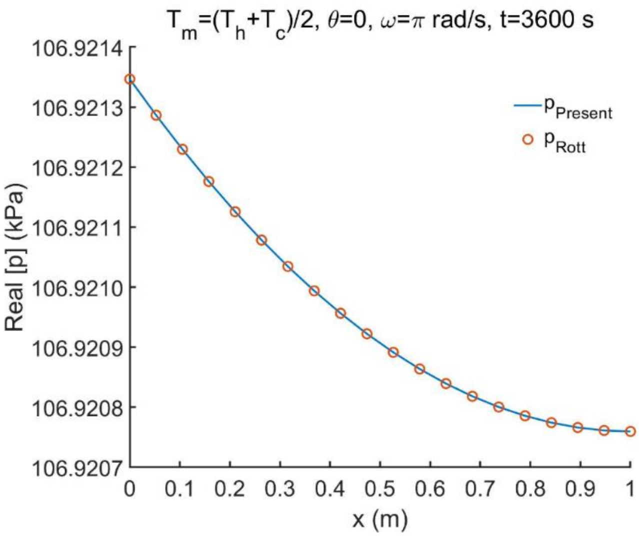

Fig. 2. Validation results for the thermoacoustic pressure

It is observed that from Fig. 2 that the results of the semi-analytical solution and the analytical solution for the thermoacoustic pressure are consistent.

Results and discussion

It is assumed that the diaphragm receives cosine excitation, so the real part of the thermoacoustic parameters is plotted and examined. In Fig. 3, the thermoacoustic pressure is plotted versus axial location for the different functions of the main flow temperature.

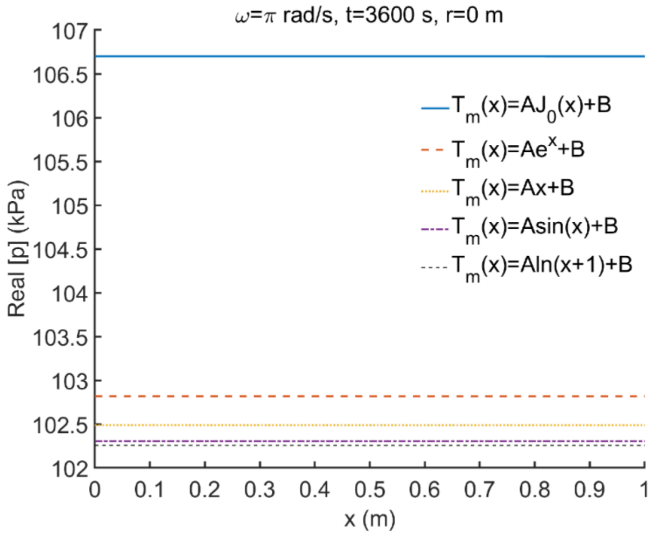

Fig. 3. Thermoacoustic pressure versus axial location for the different functions of the main flow temperature

It is observed from Fig. 3 that the thermoacoustic pressure change with axial location is not very large. The thermoacoustic pressure is a weak linear function of axial location. Therefore, thermoacoustic pressure gradient is approximately constant for different functions of the main flow temperature. On the other hand, if the main flow temperature is chosen as the Bessel function, the highest thermoacoustic pressure is achieved. Fig. 4 shows the change of centerline thermoacoustic velocity in terms of axial location for the different functions of the main flow temperature.

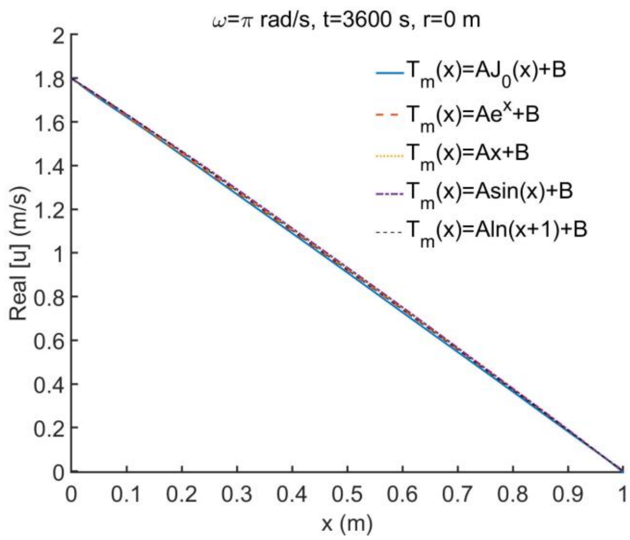

Fig. 4. Change of centerline thermoacoustic velocity in terms of axial location for the different functions of the main flow temperature

According to Fig. 4, the centerline thermoacoustic velocity varies linearly with axial location. On the other hand, the effect of the main flow temperature function on the centerline thermoacoustic velocity is small. In basic hydrodynamics knowledge, thermoacoustic velocity and thermoacoustic pressure are inversely related. The highest thermoacoustic pressure occurs for the Bessel function, so the lowest thermoacoustic velocity occurs for the Bessel function. Fig. 5 shows the change of centerline thermoacoustic density in terms of axial location for the different functions of the main flow temperature.

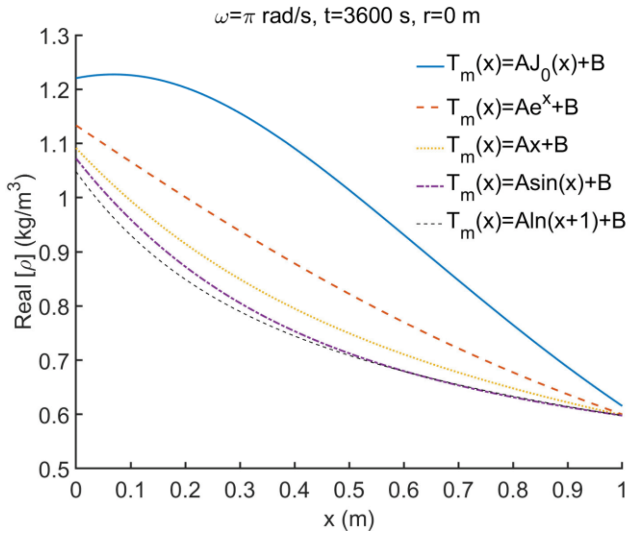

Fig. 5. Change of centerline thermoacoustic density in terms of axial location for the different functions of the main flow temperature

It is observed from Fig. 5 that the change of centerline thermoacoustic density with axial location is a decreasing function. The highest value of centerline thermoacoustic density is for the Bessel function. The centerline thermoacoustic density decreases as axial location increases. The location of the heat sink is at the beginning of the cylinder and the location of the heat source is at the end of the cylinder. Therefore, the thermoacoustic temperature at the beginning of the cylinder is lower than at the end of the cylinder, and as a result the thermoacoustic density at the beginning of the cylinder is higher than at the end of the cylinder. The change of centerline thermoacoustic temperature in terms of axial location for the different functions of the main flow temperature is shown in Fig. 6.

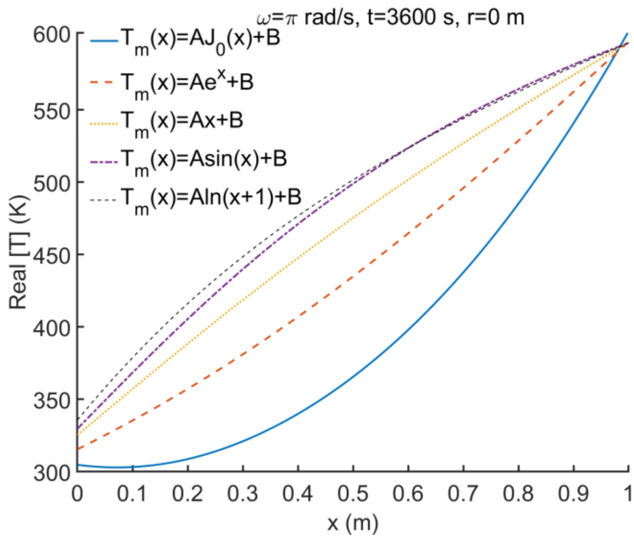

Fig. 6. Change of centerline thermoacoustic temperature in terms of axial location for the different functions of the main flow temperature

As shown in Fig. 6, the change of centerline thermoacoustic temperature with axial location is an increasing function. On the other hand, the lowest value of centerline thermoacoustic temperature occurs for the Bessel function. According to the ideal gas law, the relationship between thermoacoustic temperature and thermoacoustic density is inverse. The thermoacoustic density is maximum for the Bessel function, so the thermoacoustic temperature is minimum for the Bessel function. Fig. 7 shows the change of thermoacoustic velocity in terms of radial location for the different functions of the main flow temperature.

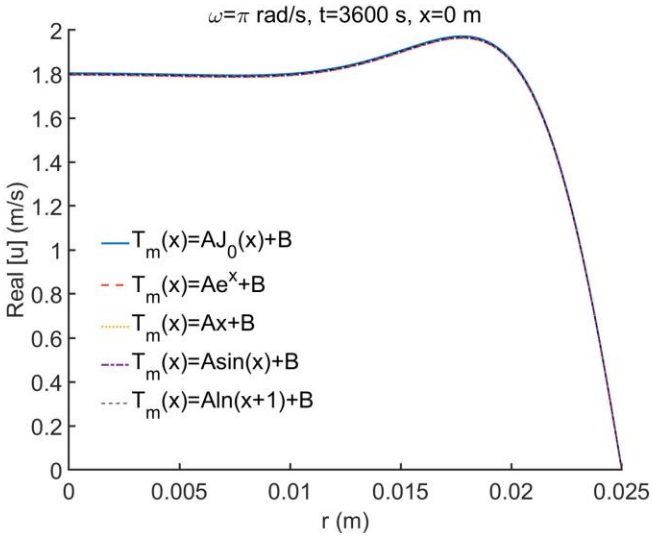

Fig. 7. Change of thermoacoustic velocity in terms of radial location for the different functions of the main flow temperature

It is observed from Fig. 7 that the effect of the function of main flow temperature on the thermoacoustic velocity is negligible. On the other hand, the velocity profile is uniform in the central region of the cylinder, but fluctuates greatly in the region near the cylinder wall due to the presence of velocity gradients. Fig. 8 shows the change of thermoacoustic density in terms of radial location for the different functions of the main flow temperature.

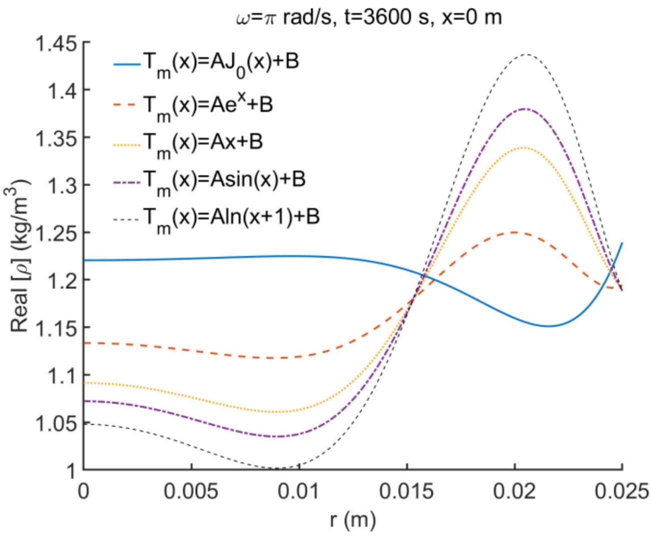

Fig. 8. Change of thermoacoustic density in terms of radial location for the different functions of the main flow temperature.

It can be seen from Fig. 8 that the largest density change occurs for the logarithmic function and the smallest density change is for the Bessel function. On the other hand, thermoacoustic density gradient is more intense near the cylinder wall than in the central region of the cylinder. Fig. 9 shows the change of thermoacoustic temperature in terms of radial location for the different functions of the main flow temperature.

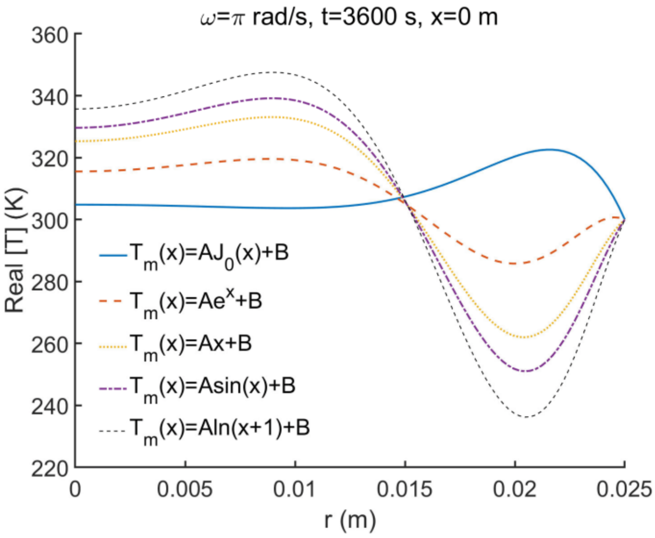

Fig. 9. Change of thermoacoustic temperature in terms of radial location for the different functions of the main flow temperature

It can be seen from Fig. 9, that the thermoacoustic temperature has the largest change for the logarithmic function and the smallest change for the Bessel function. Compared to Fig. 8, the behavior of the thermoacoustic temperature curve with radial location is the opposite of the behavior of the thermoacoustic density curve with radial location. Because according to the ideal gas law, thermoacoustic temperature and thermoacoustic density are inversely related. The gain of work flux density in terms of axial location for the different functions of the main flow temperature in Fig. 10.

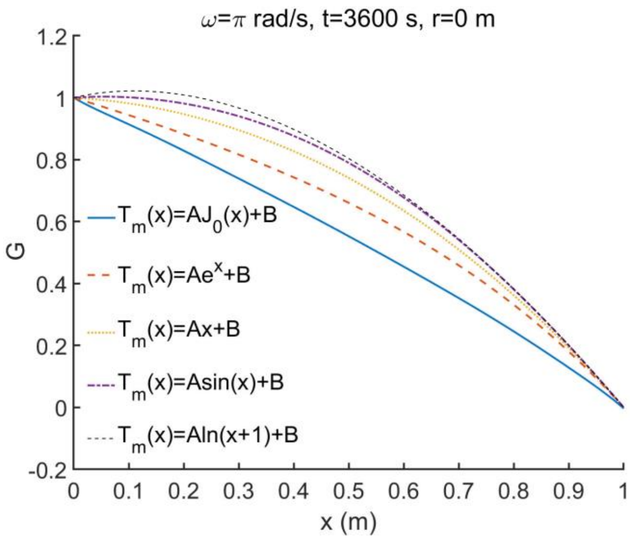

Fig. 10. Gain of work flux density in terms of axial location for the different functions of the main flow temperature

It is observed from Fig. 10 that the gain of work flux density decreases with increasing axial location. On the other hand, the highest gain of work flux density is related to the logarithmic function and the lowest gain of work flux density is related to the Bessel function. Fig. 11, shows the variation of gain of work flux density as a function of radial location for the different functions of the main flow temperature.

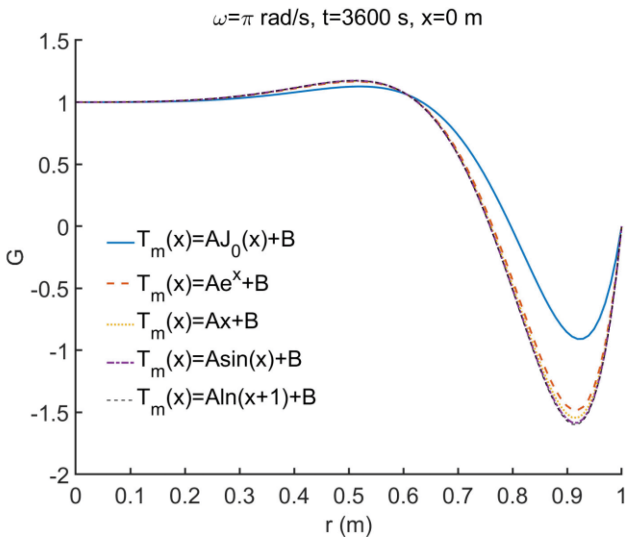

Fig. 11. Variation of gain of work flux density as a function of radial location for the different functions of the main flow temperature

It is observed from Fig. 11 that the highest absolute value of the gain of work flux density is related to the logarithmic function, and the lowest is related to the Bessel function. On the other hand, the difference in the gain value for linear function and logarithmic function is not much. However, creating logarithmic temperatures requires more economic cost. Therefore, from an engineering perspective, choosing linear temperature is more appropriate because it has lower production costs and provides relatively good gain.

Conclusion

The following conclusion obtained from the present study

- The comprehensive semi-analytical solution of the present study is capable of predicting the dynamic behavior of the thermoacoustic system under various design and operating conditions. The results of this solution are in good agreement with the analytical solution results of previous researches.
- The variation of thermoacoustic velocity with the function type of the main flow temperature is negligible.
- The thermoacoustic pressure, temperature and density change greatly with the type of the function of main flow temperature.
- The highest gain of work flux density is obtained for the logarithmic function of the main flow temperature. However, the cost of creating a logarithmic function is high from an engineering perspective.
- A linear function for the main flow temperature can provide a relatively good gain of work flux density and is easy to create from an engineering perspective.

References

[1] H. A. Kramers, Vibrations of a gas column, Physica, 15, 11-12, 971-984, 1949.

[2] N. Rott, Damped and thermally driven acoustic oscillations in wide and narrow tubes, Zeitschrift für angewandte Mathematik und Physik (ZAMP), 20, 2, 230-243, 1969.

[3] F. Wu, C. Wu, F. Guo, D. Li, Acoustically controlled heat transfer of ferromagnetic fluid, International Journal of Heat and Mass Transfer, 44, 44427-4432, 2001.

[4] W. Dai, E. Luo, G. Yu, A simple method to determine the frequency of engine-included thermoacoustic systems, Cryogenics, 46, 804-808, 2006.

[5] S. H. Tasnim, S. Mahmud, R. A. Fraser, I. Pop, Brinkman–Forchheimer modeling for porous media thermoacoustic system, International Journal of Heat and Mass Transfer, 54 ,3811-3821, 2011.

[6] E. W. S. Kam, R. M. C. So, S. C. Fu, One-step simulation of thermoacoustic waves in two-dimensional enclosures, Computers and Fluids, 140, 270-288, 2016.

[7] F. Gant, G. Ghirardo, M. R. Bothien, On the importance of time delay and noise in thermoacoustic modeling, Journal of Sound and Vibration, 501, 116067, 2021.

[8] X. Liu, L. Qin, Y. Song, J. Li, L. Yang, The effect of mean flow on the intrinsic thermoacoustic instabilities in the duct and annular combustion chambers, Aerospace Science and Technology, 127, 107691, 2022.

[9] R. Yang, J. Wang, Z. Wu, B. Huang, E. Luo, Performance analysis of thermoacoustic plasma MHD generation, Energy, 263, 125647, 2023.

[10] N. Blanc, G. Z. Ramon, Radiation-driven thermoacoustic energy conversion in absorbing media, Applied Thermal Engineering, 246, 122915, 2024.

[11] J. Huang, X. Li, H. Zhang, G. Chen, Nonlinear dynamics of a simplified subcritical thermoacoustic system under axial structure vibration, Applied Thermal Engineering, 266, 125735, 2025.

[12] A. P. Misra, Gadadhar Banerjee, Analytical and numerical study of plane progressive thermoacoustic shock waves in complex plasmas, Wave Motion, 133, 103451, 2025.

[13] M. Merk, F. Schily, W. Polifke, A Jacobian-based framework for the derivation of comprehensive thermoacoustic jump conditions, Combustion and Flame, 274, 113958, 2025.

[14] P. Merkli, H. Thomann, Thermoacoustic effects in a resonance tube, Journal of Fluid Mechanics, 70 (1),161-177, 1975.

[15] M. Senga, S. Hasegawa, Energy conversion of thermoacoustic engines with evaporation and condensation, International Journal of Heat and Mass Transfer, 165, 120385, 2021.

[16] L. F. Shampine, J. Kierzenka, M. W. Reichelt, Solving boundary value problems for ordinary differential equations in MATLAB with bvp4c, WashU McKelvey School of Engineering, 2000, Available at https://classes.engineering.wustl.edu/che512/bvp_paper.pdf; Access: December 2024.